https://doi.org/10.5194/egusphere-2025-6244
Preprint. Discussion started: 19 February 2026

Spatially variable wildfire impacts on sediment mobilization: event-scale evidence from eastern Australian catchments

Danlu Guo[1,2●], Qian Wang[1,2●], Peter B. Hairsine[3]

[1]School of Engineering, College of Systems and Society, The Australian National University, Canberra, ACT, Australia
[2]Institution for Water Futures, Australian National University, Canberra, ACT, Australia
[3]The Fenner School of Environment and Society, College of Systems and Society, Australian National University, Canberra, ACT, Australia
●These authors contributed equally to this work.

Correspondence to: Danlu Guo (danlu.guo@anu.edu.au); Qian Wang (Qian.Wang2@anu.edu.au)

Abstract. Wildfires may profoundly affect forested catchments by altering hydrological processes, soil properties, and sediment dynamics. While post-fire increases in water quality constituents are well documented, the underlying divers for such changes remain poorly understood. This study examines how fire and short-term hydrologic conditions interact to shape sediment dynamics using a novel Bayesian Hierarchical modelling framework. The analysis is at event-scale based on multi-year, high-frequency turbidity and streamflow data collected from 14 forested catchments in eastern Australia, which were burned to varying severities during the 2019/2020 Black Summer fires and affected by subsequent floods. Further, we explored how these effects vary across catchments with the extent of burning and other catchment characteristics.

Model results show that severe burning had a clear steepening effect on the slopes of event concentration-discharge (C-Q) in 5 out of the 10 severely burnt catchments studied, indicating enhanced sediment mobilization following extreme burning. The influence of short-term hydrologic conditions on C-Q slopes was comparatively minor, suggesting that fire effects dominated post-disturbance sediment responses. The magnitude of fire effects (as post-fire changes in the C-Q slopes) did not always scale directly with the proportion of catchment burnt, which also seems to be driven by the location of extreme burning and forest types. These findings provide a large-scale, multi-catchment understanding of post-fire sediment mobilization mechanisms, which can inform future improvement of modelling and management of sediment in fire-affected forested landscapes.

https://doi.org/10.5194/egusphere-2025-6244
Preprint. Discussion started: 19 February 2026

1 Introduction

Wildfires – commonly regarded as extreme events – are occurring with increasing frequency and intensity (Cunningham et al., 2024). These events can alter the hydrological and biogeochemical processes in forested catchments, including reduced canopy interception, increased soil erodibility, and loss of surface cover together enhance runoff and sediment mobilization (Meyer et al., 2001; Shakesby, 2011; Nolan et al., 2014). These effects can together lead to elevated levels of river pollutants such as sediments and nutrients and may degrade stream habitats (Hampton et al., 2022; Raoelison et al., 2023).

Existing literature has widely recognized impacts of fire on the measured water quality attributes, including temperature, turbidity, sediment, nutrients, major ions, etc. (Smith et al. 2011; Mast et al. 2016; Chen and Chang 2023; Marcotte et al. 2024). Key post-fire changes in water quality include elevated levels of exports and concentration metrics (e.g., maximum and average values) of suspended sediment and nutrients (e.g., total nitrogen and total phosphorus) in streams (Hampton et al. 2022), particularly in the first year after fire (Smith et al. 2011). Some changes could be observed up to five years after fire on average (Rust et al. 2018). The extent of the fire-induced impacts on water quality is driven by multiple factors which arise from catchment characteristics (Reale et al. 2015; Hall et al. 2022; Marcotte et al. 2024), hydro-climate conditions (Sherson et al. 2015; Mast et al. 2016; Hall et al. 2022; Johnston and Maher 2022; Richardson et al. 2024), and fire properties (Smith et al. 2011; Raoelison et al. 2023; Richardson et al. 2024; Brown and Hunt 2025).

While post-fire changes in water quality constituents are well documented, understanding of the processes governing pollutant transport patterns remain limited. Some recent studies have extended the attention to the concentration-discharge (C-Q) relationship, as they provide insights into the watershed hydrology and biogeochemistry connections and the water quality dynamics. The key changes include distorted C-Q relationships during initial hydrograph peaks post-fire (Johnston and Maher 2022), stronger enrichment trends or weaker dilution trends in C-Q slopes, depending on the constituents (Richardson et al. 2024), and upward shifted C-Q regression lines for solutes derived mainly from weathering (Clow et al. 2024).

C-Q relationships are inherently highly variable across space and time, reflecting differences in catchment characteristics and hydrological regimes. Spatial variability is driven by factors such as land use, management, lithology, and topography (McGuire et al., 2014; Jensen et al., 2019; Minaudo et al., 2019; Ebeling et al., 2021; Dupas et al., 2021), while temporal variability reflects sediment source availability and the balance between baseflow and quickflow (Moatar et al., 2017; Minaudo et al., 2019; Gorski and Zimmer, 2021; Knapp et al., 2022). The proportion of baseflow contribution also explains spatial differences in C–Q patterns across many catchments (Guo et al., 2023). Wildfire further amplifies these variabilities. Event-scale features such as hysteresis and flushing indices often shift after fire (Mast et al., 2016; Marcotte et al., 2024), yet these changes are difficult to resolve with discrete sampling, which commonly misses highly dynamic post-fire responses (Richardson et al., 2024). Consequently, few studies have quantified (1) the relative influence of wildfire compared with other key drivers of C–Q behaviour, and (2) how fire effects vary spatially across catchments.

To address this gap, this study aims to assess the impacts of wildfire and short-term hydrological conditions on sediment mobilization for forested catchments. This is facilitated by the recent increases in the availability of high-frequency monitoring

https://doi.org/10.5194/egusphere-2025-6244
Preprint. Discussion started: 19 February 2026

data enabling a regional event-scale analysis. We focus on a regional study of eastern Australia which underwent unprecedented wildfires in 2019-2020, with almost half of the high-severity fires recorded in the past three decades and severe burning affecting over 14% of native woody vegetation (Collins et al., 2021), with demonstrated impacts on catchment hydrology (e.g., Guo et al., 2023). In this instance, the post-fire period contained large-scale flooding across much of eastern Australia (Kemter et al., 2021). These combined features make the region an interesting case to explore the interacting effects of fire and hydrological changes. We hypothesize that the extreme burning and recent hydro-climatic conditions (e.g., streamflow, catchment wetness) jointly shaped the sediment mobilization in forested catchments.

2 Data and Methods

2.1 Study sites and data

This regional analysis was conducted across 14 forested catchments (each with forest covering at least 50% of the catchment area) in eastern Australia which experienced various severity of burning during the 2019/2020 fire season (Fig. 1). When summarizing burning severity at the catchment scale, we used a threshold of 0.1% of the catchment area experiencing extreme burning to differentiate extremely burnt catchments from non-extremely burnt catchments. We selected this threshold to assert that changes in sediment sourcing and hydrological behaviour (as described in the Introduction) are triggered by extreme burning, consistent with previous studies highlighting the role of fire severity (e.g., Rhoades et al., 2011; Khaledi et al., 2022; Marcotte et al. 2024). This assertion was verified by including the percentage area of extreme burning as a factor in the subsequent analysis of spatial variation of the fire effects (Sect. 2.4).

Key criteria used to inform the catchment selection are presented below, with the definition of burning severity introduced subsequently:

1. Each catchment has maintained high-frequency (hourly) monitoring of turbidity and streamflow covering the period of 1.5 years before and after Oct 25, 2019, which broadly marks the start of the 2019/2020 fire season for the region. This ensures sufficient data from both the pre- and post-fire periods for analyzing sediment mobilization for each catchment.
2. No more than 0.1% of each catchment experienced extreme burning during any of the 2017/2018 and 2018/2019 seasons. This ensures minimal effect of prior burning on the study catchments which might interfere with the 2019/2020 fire effects that this study focuses on.
3. Further, the locations catchment outlets were checked and ensured none is immediately downstream of large waterbodies or artificial dams/weirs. This minimizes possible modulation of sediment mobilization from large waterbodies or anthropogenic infrastructures.

https://doi.org/10.5194/egusphere-2025-6244
Preprint. Discussion started: 19 February 2026

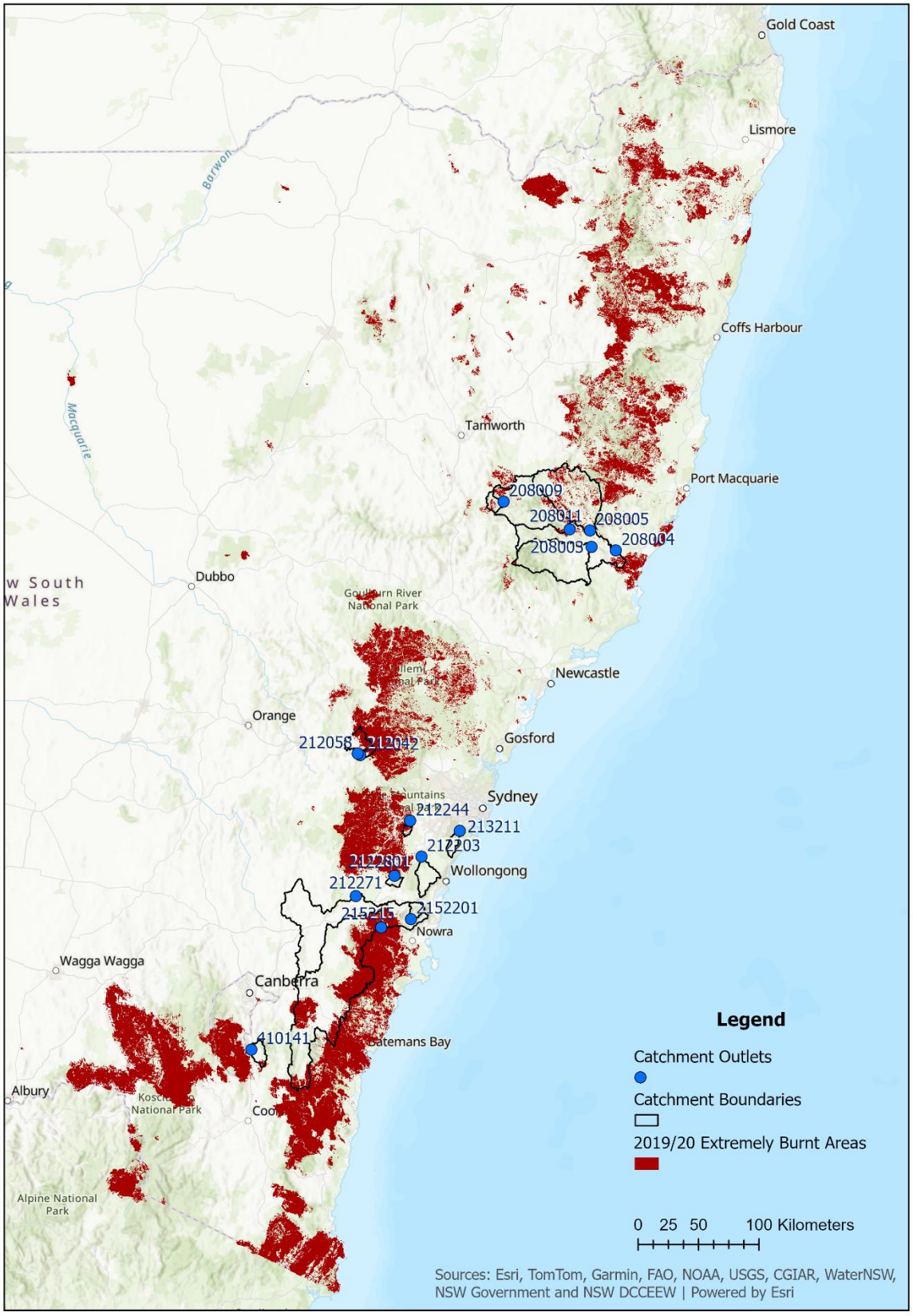

https://doi.org/10.5194/egusphere-2025-6244
Preprint. Discussion started: 19 February 2026

Figure 1: Map of the 14 study catchments identified by their outlets (where flow and turbidity were measured) and boundaries, within eastern Australia. The dark red shaded region shows the extent of area being extremely burnt in the 2019/2020 wildfire. Extreme burning was defined following the NSW Fire Extent and Severity Mapping dataset for the 2019/2020 fire season (NSW Government and NSW DCCEEW, 2021)

Based on the catchment selection criteria above, and the proportional catchment areas experienced extreme burning during the 2019/2020 season, our catchment selection resulted in:

- 10 *extremely burnt catchments*, which experienced extreme burning over ≥0.1% proportional catchment areas during the 2019/2020 fire season;
- 4 *non-extremely burnt catchments*, which experienced extreme burning over <0.1% proportional catchment areas during the 2019/2020 fire season.

The percentage of extreme burning for each catchment in the 2019/2020 fire season, along with the 10 extremely burnt catchments and the 4 non-extremely burnt catchments, are listed in Table 1. Proportional catchment areas with other fire severities than 'extreme' (i.e., high, moderate, low and unburnt) are also presented

Table 1: List of the 14 study catchments and their corresponding percentage areas being burnt with different severity in 2019/2020 fire, extracted from the NSW Fire Extent and Severity Mapping dataset for the 2019/2020 fire season (NSW Government and NSW DCCEEW, 2021). Shaded cells highlight the 10 extremely burnt catchments.

Catchment ID	Percentage area being burnt with different severities, in the 2019/2020 fire season				
	Extreme	High	Moderate	Low	Unburnt
208003	0.1	0.3	0.3	0.2	99.2
208004	1.1	1.7	10.2	7.4	80.0
208005	1.9	2.7	24.5	19.7	51.2
208009	1.5	1.3	10.1	5.1	82.1
208011	1.1	1.4	6.7	3.0	87.8
212042	13.8	20.0	18.3	4.8	43.1
212058	14.2	10.9	13.0	3.2	58.7
212203	0	0	0	0	100
212244	7.4	15.1	17.9	11.5	48.1
215215	15.2	7.3	6.0	6.4	65.3
410141	1.5	4.0	3.0	2.3	89.2
213211	0	0	0	0	100
2122801	0	0	1.2	0.9	97.9
2152201	0	0	0	0	100

https://doi.org/10.5194/egusphere-2025-6244
Preprint. Discussion started: 19 February 2026

To support the above catchment selection and fire severity estimation, data were acquired from multiple sources summarized in Table 2. Besides, the locations of catchment outlet relative to large water bodies and dams/weirs (described in the above catchment selection Criteria 3), were visually checked using the maps of turbidity/streamflow monitoring sites provided by the WaterNSW continuous water monitoring network portal at https://realtimedata.waternsw.com.au/water.stm (WaterNSW, 2020).

Table 2: Key datasets and sources to support the study catchment selection

Data	Description	Data source and summary
Turbidity and streamflow data	These data were first examined to filter out catchments by data availability (described in the above Criteria 1). Further, these data formed the basis of analyzing sediment export patterns pre- and post-fire (detailed in Sect. 2.2).	Hourly data for for all catchments were sourced from the WaterNSW continuous water monitoring network portal: https://realtimedata.waternsw.com.au/water.stm (WaterNSW, 2020).
Forest cover	This dataset was used to map the forest extent to identify the forested catchments analysed (i.e., with ≥50% catchment area covered by forest) above.	The National Forest and Sparse Woody Vegetation Data (Version 4, 2019 Release): https://data.gov.au/data/dataset/national-forest-and-sparse-woody-vegetation-data-version-4-2019-release (Department of Industry, Science, Energy and Resources, 2019), in 25-metre resolution and representing the 2019 condition.
Burning severity	This dataset was used to map locations of extreme burning in the 2017/2018, 2018/2019 and 2019/2020 seasons for 1) differentiating the extremely burnt and non-extremely burnt catchments for the 2019/2020 season; and 2) check for any prior residual fire effects described in the above Criteria 2.	Annual layers of the NSW Fire Extent and Severity Mapping (FESM) dataset: https://datasets.seed.nsw.gov.au/dataset/fire-extent-and-severity-mapping-fesm For each fire season (e.g., 2019/2020, 2018/2019, 2017/2018), the dataset included mappings of all wildfires burning over 10ha from July of the starting year to the June of the ending year (NSW Government and NSW DCCEEW, 2020a, 2020b, 2021).
Catchment boundaries	This dataset was used to clip the fire severity data and forest extent data to individual catchments to calculate the proportional	The boundaries were delineated from the locations of the turbidity/streamflow monitoring sites (obtained from the WaterNSW continuous water monitoring network portal

https://doi.org/10.5194/egusphere-2025-6244
Preprint. Discussion started: 19 February 2026

	coverages, as well as clipping the catchment-scale data used in explaining the spatial variation of modelled fire effects (detailed in Sect. 2.4).	along the streamflow and turbidity data), based on the national 1 second Smoothed Digital Elevation Model (DEM-S) data (https://ecat.ga.gov.au/geonetwork/srv/eng/catalog.search#/metadata/72759, Gallant et al., 2011) via ArcGIS Pro.

2.2 Preliminary analyses

Prior to the formal modelling process, preliminary analysis was performed to provide an overview of post-fire changes of turbidity and flow conditions across sites and reveal any spatial patterns in these changes. In specific, we compared the pre- and post-fire turbidity and discharge levels, as well as the event-scale C-Q slopes as an indication of sediment mobilization.

To assess the event-scale C-Q relationships, we focused on paired C-Q data within the storm event periods only. In this data preparation process, it is noted that the choice of pre- and post-fire periods (1.5 years before and after the fire occurrence, see Sect. 2.1) generally resulted in too few events pre-fire relative to the post-fire period across all catchments, which is likely due to the drier conditions before fire. As such, the final pre-fire period for each catchment has been extended to 2.5 years before the fire.

To identify periods within and outside of streamflow events, R package *hydroEvents* (https://cran.r-project.org/web/packages/hydroEvents/index.html) (Wasko and Guo, 2022) has been employed, as it provides a consistent statistical framework to identify events from long-term, multi-catchment datasets. The *eventMaxima* method has been used, which defines an event by identifying a local maximum in the streamflow time series that exceeds a specified threshold relative to the surrounding minima. This method was found to be the most robust statistical event identification approach for when user-specified rules are required to define events (Mohammadpour Khoie et al., 2025). The *eventMaxima* method requires baseflow separation a priori, for which, we applied the Lynn and Hollick recursive digital filter (Ladson et al., 2013) with an alpha of 0.98, via the *baseflowB* function in the same package. The choice of the alpha value is consistent with the typical literature recommendation (Wasko and Guo, 2022), as well as aiming to align with the findings in Jaffrés (2021) that long-term BFI at sites in NSW tends to be smaller than 0.5.

Following the streamflow event identification, visual comparison and the Mann-Whitney U test (also known as the Wilcoxon rank-sum test) were used to compare whether there are significant differences in distributions of discharge, turbidity, and event-scale C-Q slopes, between the pre- and post-fire periods. The test is a non-parametric statistical test used to compare differences between two independent groups and particularly useful when the data is not normally distributed. The null hypothesis used in this work is that variables compared before and after fire have the same distribution.

https://doi.org/10.5194/egusphere-2025-6244
Preprint. Discussion started: 19 February 2026

2.3 Modelling processes

We used a Bayesian hierarchical modelling framework to identify the key drivers of sediment mobilization amongst fire disturbances and recent hydrological conditions, across all study catchments. This modelling framework has been demonstrated powerful to interpret water quality and ecological data across multiple catchments, allowing 'information sharing' across groups and/or catchments while maintaining spatial heterogeneity in key patterns and dynamics (Webb and King, 2009; Guo et al., 2018, 2020, 2023).

2.3.1 Overview and model structure

The model focused on the event-scale C-Q relationships to represent sediment export. We describe event-scale C-Q relationships with a simple power-law C-Q model for each catchment, as:

$$C_{S,e,t} = a_{S,e} \times (Q_{S,e,t})^{b_{S,e}} \quad (1)$$

$$\text{which is equivalent to } \log(C_{S,e,t}) = a_{S,e} + \log(Q_{S,e,t}) \times b_{S,e} \quad (2)$$

where S indicates each site or catchment. For each site S, within each event e, t is the index of paired C-Q samples within the event in time order, C is hourly turbidity (NTU), Q is hourly streamflow (cubic meter per second), a and b are event-specific parameters defining the event-scale C-Q relationship.

Eqn. 2 makes the first layer of the Bayesian hierarchical model. The event-scale C-Q slopes, $b_{S,e}$, become the predictands for the second layer, while the selection of predictors (discussed subsequently) intends to capture the potential impacts of intense wildfire and key indicators of recent hydrological conditions that control sediment sourcing and mobilization from catchments to waterways.

Note that while post-fire hydrological changes are well documented (e.g., Nolan et al., 2014; Khaledi et al., 2022), the concurrent period of widespread flooding in eastern Australia (Kemter et al., 2020) makes it analytically challenging to disentangle fire effects from hydrology-driven changes. Since wildfire and hydrological conditions interact and are not statistically independent, a two-step regression approach (e.g., first estimating the influence of fire on hydrological variables, then relating those hydrological responses to sediment export) would risk confounding their effects and obscuring their joint influence. This challenge motivated our modelling approach, which explicitly examines how C-Q slopes are jointly modulated by wildfire and short-term hydrological conditions. Following this rationale, this second layer to predict the event-scale C-Q slopes is formulated as Eqn. 3 for each catchment, and explained with its predictors justified subsequently.

$$b_{S,e} = inter_{S,b_e} + \beta_{S,Q_{lastvolume}} \times Q_{S,lastvolume_e} + \beta_{S,Q_{thisvolume}} \times Q_{S,thisvolume_e} + \beta_{S,timesincelast} \times S.timesincelast_e + \beta_{S,if\_afterfire} \times S.if\_afterfire_e \quad (3)$$

In which, for each site S:

- $b_{S,e}$: event C-Q slopes for each event e at site S, as in Eqn. 2;
- $Q_{S.lastvolume\_e}$: total flow volume over the previous storm event; indicating whether the sediment is likely flushed out prior to the current event;

https://doi.org/10.5194/egusphere-2025-6244
Preprint. Discussion started: 19 February 2026

- $Q_{S,thisvolume\_e}$: total flow volume overt the current storm event; indicating the likely sediment mobilization for the current event;
- *S.timesincelast_e*: time (in days) since previous storm event, till the start of the current event); this is an indicator of the likely accumulation of sediments in the catchment prior to the current event;
- *S.if_afterfire_e*: fire occurrence, represented with binary values indicating whether current storm event is before (0) or after (1) fire;
- β terms represent the site-specific effect of each abovementioned potential driver of event C-Q slopes;
- $inter_{S,be}$ is the site-specific regression interception term, representing the expected event C-Q slope where $Q_{S,thisvolume}$, $Q_{S,lastvolume}$ and *S.timesincelast_e* all take the mean of the site, within the pre-fire period (i.e., all of standardized $Q_{S,thisvolume}$, $Q_{S,lastvolume}$ and *S.timesincelast_e* are 0, and *S.if_afterfire_e* = 0 – see the subsequent subsection for data standardization).

2.3.2 Model calibration

The above Eqns. 2 and 3 constitute the key formulae for the Bayesian hierarchical model used in this study. The benefit of the Bayesian hierarchical modelling framework is that, instead of calibrating model parameters separately for each event, it allows event-specific parameters to be drawn from a common distribution across multiple events. Further, the catchment-specific β terms can also be drawn from a common distribution across catchments. Adopting this hierarchical modelling approach means that our analyses could maximizes the 'borrowing strength' across observations from individual events and catchments, in line with the proven efficiency of such framework in drawing information from limited data (e.g., Guo et al., 2018, 2023).

In Eqn.3, fire occurrence (*S.if_afterfire_e*) is binary variable (only taking values of 0 or 1). The remaining three predictors for the event C-Q slopes – $Q_{S,lastvolume}$ and $Q_{S,thisvolume}$ representing the volume of the last and current flow events, and *S.timesincelast* representing days since last flow event – have all been log transformed to improve the data normality. The transformed variables have been further standardized for each catchment, so that they have a mean of 0 and a standard deviation of 1 for each catchment. This standardization ensured that once calibrated, all model parameters (β) are in a similar range and can be comparable across different drivers.

The model calibration was done in R with package *rstan* (Stan Development Team, 2025). *rstan* carries out Bayesian calibration by using Markov chain Monte Carlo to sample from the posterior distribution, combining the prior information with the likelihood of the observed data to obtain parameter estimates. All site-level predictors for the event C-Q slopes ($inter_{S,be}$, $\beta_{S,Qlastvolume}$, $\beta_{S,Qthisvolume}$, $\beta_{S,timesincelast}$ and $\beta_{S,if\_afterfire}$, in Eqn.3) were drawn from hyperprior distributions shared across sites. All hyper parameters and parameters were given weakly informative priors to allow a broad range of possible magnitudes, specifically, a *Exp(1)* prior is assigned for positive-only parameters (the normal standard deviation terms) and a *N(0,1)* is assigned for unconstrained parameters (the normal mean terms). Because all predictors were standardized, this prior implies that most coefficients are expected to fall within approximately ±3 on the standardized scale, which prevents overfitting while remaining broad enough to accommodate substantial effects if supported by the data. We used four independent Markov chains in each model run, with a total of 4000 model iterations for each chain. Convergence of the chains was ensured by checking the *Rhat* value (Sturtz et al., 2005) – an *rstan* output that suggests sufficient mixing of the four independent Markov chain, and

https://doi.org/10.5194/egusphere-2025-6244
Preprint. Discussion started: 19 February 2026

thus convergence of calibration. An *Rhat* value of below 1.1 was used as the convergence threshold (Stan Development Team, 2018). The full modal formulations and the *rstan* codes are included in Fig. A1, Appendix A.

2.4 Model evaluation and inferences

Once calibrated, we first evaluated the model performance on whether it can satisfactorily represent the observed variability in turbidity. Then we assessed the posterior distribution of each β term in Eqn. 3 to interpret the effects of fire and catchment hydrological conditions on the C-Q slopes for individual catchments. Following these assessments, we can recommend whether the fire has significantly shifted the C-Q slopes, as well as the relative importance of the key drivers shaping the C-Q slopes (i.e., fire and hydrological conditions).

As a final investigation, we explored how the effect of fire changes across the extremely burnt catchments. The effect of fire was with the median of posterior $\beta_{S,if\_afterfire}$ values (Eqn. 3) for individual catchments, representing the modelled, catchment-specific post-fire change in event C-Q slopes attributed to fire. The effect of fire was then correlated to a comprehensive set of catchment-scale characteristics on geography, burning characteristics and forest characteristics, listed and justified in Table 3.

Table 3: Catchment-scale characteristics to explore how the fire effects changes across space.

Category	Catchment-scale characteristics	Description	Justification
Geography	*Catchment area*	Total catchment area (in km^2). This was estimated with ArcGIS with the catchment boundaries delineated in earlier steps.	This represents any scale effects of the fire-induced changes in C-Q slopes.
	% Sand topsoil	Percentage of sand in the topsoil layer (0-5cm). Spatial data were obtained from the Soil and Landscape Grid National Soil Attribute Maps - Sand (3" resolution) - Release 2 (https://data.csiro.au/collection/csiro:55735, Malone et al ., 2022), clipped to each catchment.	This is included considering that sandy materials are highly susceptible to developing post-fire hydrophobicity and subsequent erosion.
Burning characteristics	*% Extreme burnt*	Percentage of catchment area being extremely burnt in 2019/2020 season. This was estimated with the extremely burnt areas for 2019/2020 (from the NSW Fire Extent and Severity Mapping dataset), clipped to each catchment.	This variable combines measures of percentage of burnt area and burnt severity within catchment. The former was found to be an important control of the post-fire changes in runoff ratio across temperate forests in Australia (e.g., Khaledi et al., 2022). The latter was chosen to focus on extreme burning (full

https://doi.org/10.5194/egusphere-2025-6244
Preprint. Discussion started: 19 February 2026

			canopy consumption, as defined in the dataset), which is expected to produce substantially higher sediment inputs and greater modulation of hydrological processes.
	Normalized distance to outlet	Mean distance between each pixel of the extremely burnt area in 2019/20 season within each catchment and the corresponding catchment outlet (i.e., where turbidity and streamflow are monitored). The distance in km is normalized by the square root of catchment area to account for scaling effect.	This variable is included as a source of erosion that is closer to the outlet of the catchment is less subject to changes in storage of sediment in catchment (e.g. with footslopes and channel benches).
Forest formation types (mapped in 2018)	*% Non-forest*	Percentage of catchment area not occupied by forest (mapped in 2018) Spatial data of forest formation (i.e., classifications of forest combining type, covering and height) were sourced from the Forests of Australia dataset, clipped to each catchment (ABARES, 2018). The subsequent forest types are sourced from the same dataset.	Forest characteristic has been demonstrated to affect the post-fire responses of catchment hydrology (e.g., Kuczera, 1987; Vertessy et al., 2001; Webb and Jarrett, 2013). The selected forest formation types are informed by key types present across the study catchments (i.e., with >0 coverage for most study catchments).
	% Acacia	Percentage of catchment area occupied by acacia forest	
	% Eucalypt medium woodland	Percentage of catchment area occupied by Eucalypt medium (height between 10-30m) woodland (forest crown cover between 20-50%)	
	% Eucalypt medium open	Percentage of catchment area occupied by Eucalypt medium (height between 10-30m) open (forest crown cover between 50-80%)	
	% Eucalypt tall open	Percentage of catchment area occupied by Eucalypt tall (height over 30m) open (forest crown cover between 50-80%)	
	% Eucalypt low woodland	Percentage of catchment area occupied by Eucalypt low (height between 2-10m) woodland (forest crown cover between 20-50%)	

https://doi.org/10.5194/egusphere-2025-6244
Preprint. Discussion started: 19 February 2026

	% Other native forest	Percentage of catchment area occupied by other native forest types	
	% Rainforest	Percentage of catchment area occupied by rainforest	

3 Results

3.1 Event-scale comparison of pre- and post-fire sediment levels and export patterns

Fig. 2 compares the pre- and post-fire turbidity and discharge during storm events for each catchment, grouped by the extremely burnt catchments (panels a, c) and the non-extremely burnt catchments (panels b, d). Post-fire discharge demonstrates a consistent increase across both the extremely burnt and non-extremely burnt catchments (Fig. 2c, d), with significant increases observed in all but two catchments (one extremely burnt and one non-extremely unburnt).

In contrast, post-fire turbidity has shown systematic increases only for the extremely burnt catchments (Fig. 2a), with 9 out of 10 catchments saw significant increases. None of the non-extremely burnt catchments observed significant increase (Fig. 2b), while post-fire turbidity levels remain similar or slightly lower than the corresponding pre-fire levels.

https://doi.org/10.5194/egusphere-2025-6244
Preprint. Discussion started: 19 February 2026

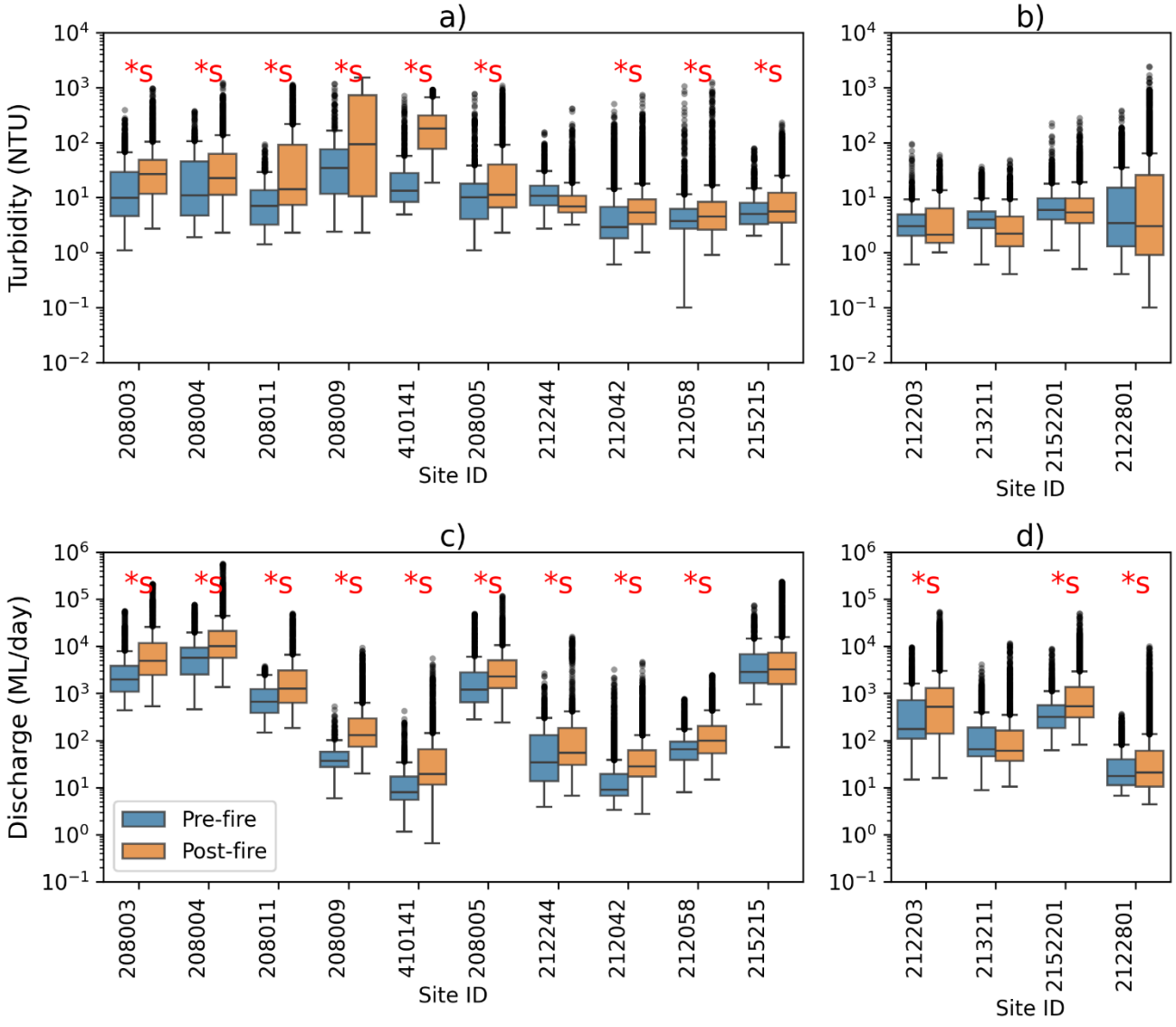

Figure 2: Boxplots of turbidity during storm events of pre and post fires across a) extremely burnt and b) non-extremely burnt sites; and for discharge during storm events of pre and post fires across c) extremely burnt and d) non-extremely burnt sites. *s represents p < 0.05 from the Mann-Whiteney U test, indicating that the pre- and post-fire turbidity distributions are significantly different, with the former smaller than the latter.

Further comparisons were also carried out for the event-scale sediment export between the pre- and post-fire periods of each catchment by examining the C-Q relationship (Fig. 3), across a) extremely burnt catchments and b) non-extremely burnt catchments. In contrast with the systematic post-fire increase in turbidity across the extremely burnt catchments in Fig. 2a, the

https://doi.org/10.5194/egusphere-2025-6244
Preprint. Discussion started: 19 February 2026

changes in the export pattern in these extremely burnt catchments (Fig. 3a) demonstrate no systematic shift from pre- to the post-fire period. Further statistical test of differences between the pre- and post-fire groups of event-scale C-Q slopes (Fig. 4a) shows that there is no universal post-fire increases in the C-Q slopes for the extremely burnt catchments, with significant
240 increase only seen at one catchment (208004). None of the non-extremely burnt catchments has a significant increase in the event C-Q slopes after fire (Fig. 4b).

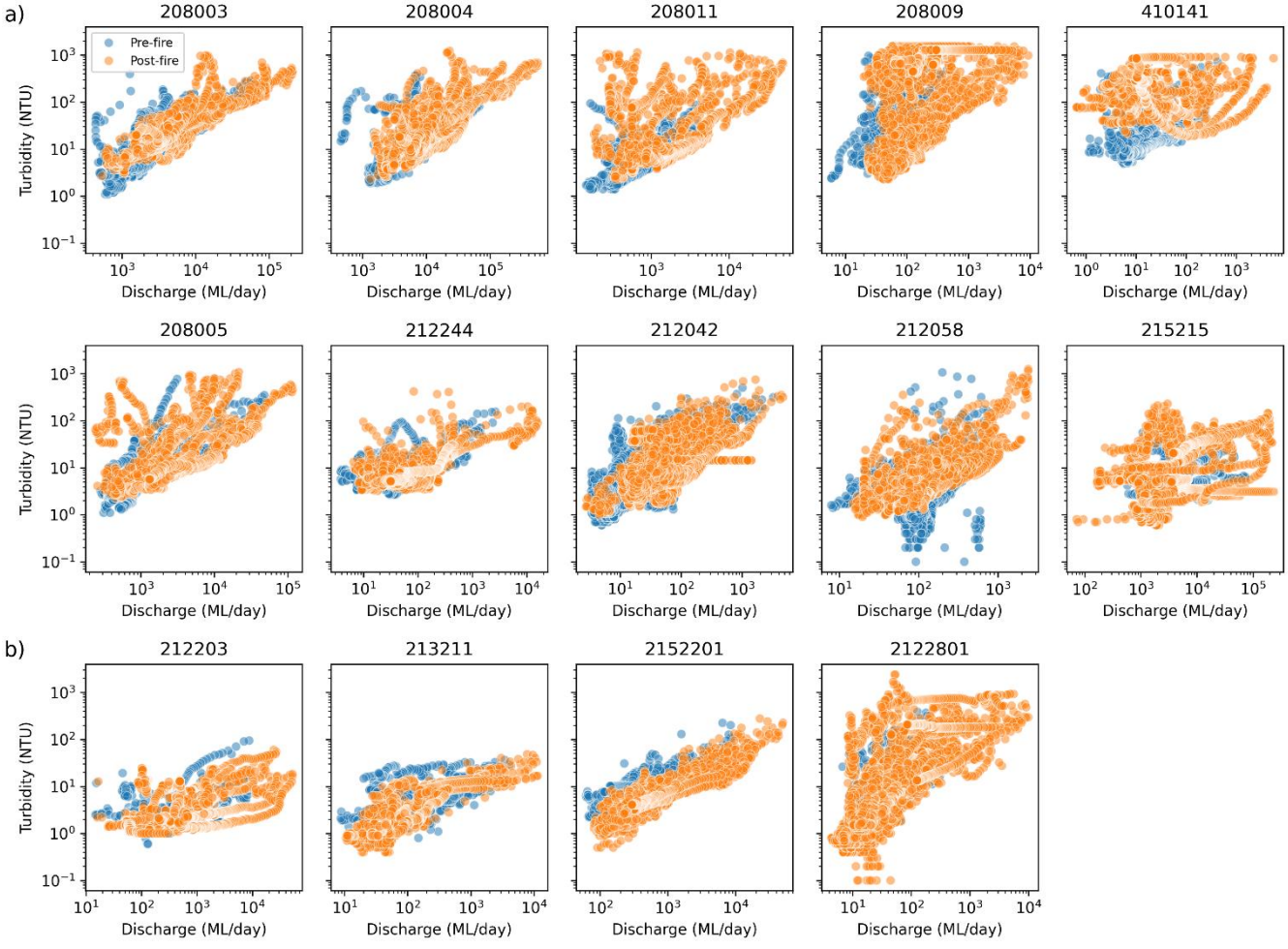

Figure 3: Turbidity-flow (y-x) relationships pre-fire and post-fire, during events only, where a) for extremely burnt catchments and b) for unburn catchments.

https://doi.org/10.5194/egusphere-2025-6244
Preprint. Discussion started: 19 February 2026

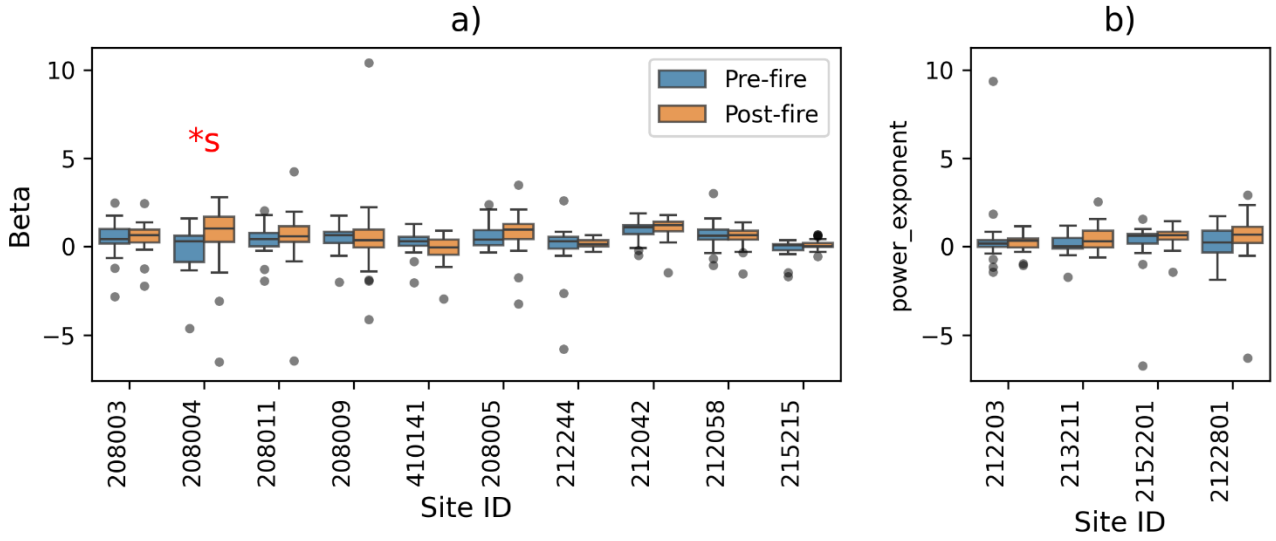

Figure 4: Distribution of event-scale C-Q slopes (Beta) for each catchment, before and after fire, for a) extremely burnt catchments; b) non-extremely burnt catchments. Each box summarizes the distribution of event C-Q slopes across the number of events within the pre- and post-fire periods for each catchment. *s represents $p < 0.05$ from Mann-Whiteney U test, indicating that the pre- and post-fire Beta distributions are significantly different, with the former smaller than the latter.

While the above results give initial indication on the likely post-fire changes in sediment mobilization, as also demonstrated, the post-fire period seems to associate with higher flows, as well. Quantifying potential effects from the fire itself or due to changes in the hydrological conditions would recommend the relative importance of these drivers in modulating sediment mobilization, which is demonstrated by the subsequent modelling results.

3.2 Modelled effects of fire and hydrological conditions on sediment mobilisation

Fig. 5 shows all posterior simulation of turbidity from this Bayesian hierarchical model, against the observed turbidity in log space. The model demonstrates satisfactory performance in explaining the observed variability in log10-transformed turbidity, with a median Nash-Sutcliff Efficiency (NSE) of 0.85 across all posterior samples indicating 85% variability explained. Further, in the raw measurement space (untransformed), the median NSE is 0.554 also demonstrating good predictive ability although with also notable impact of data skewness. The strong predictive performance provides confidence in proceeding to interpret the model inferences i.e., the modelled effects of fire and hydrological conditions on the C-Q slopes.

https://doi.org/10.5194/egusphere-2025-6244
Preprint. Discussion started: 19 February 2026

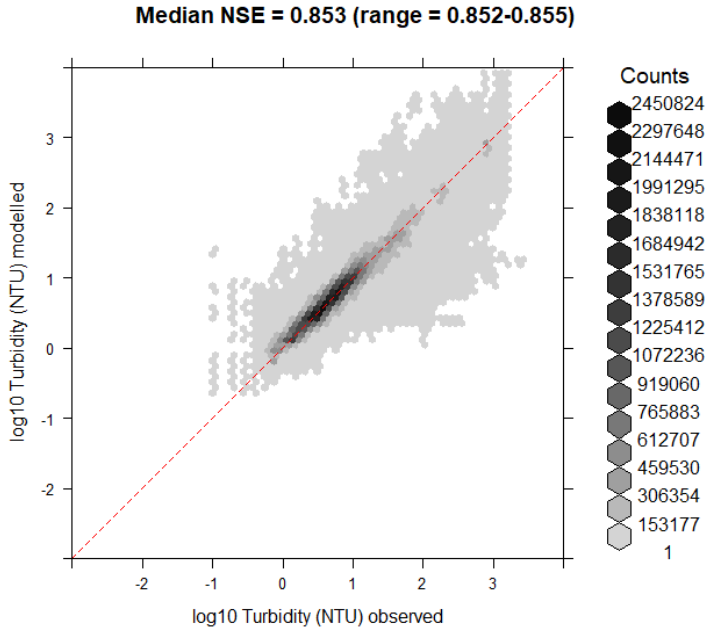

Figure 5: Performance of the Bayesian hierarchical models across all 14 study catchments, represented by the full posterior simulations (y-axis) plotted against the observed turbidity (x-axis) in log space. Darker regions represent denser distribution of values of simulations and observations. The median and range of Nash-Sutcliffe Efficiencies across all posterior model simulations is shown above the plot.

3.2.1 Effects of fire on event C-Q slopes

Fig. 6 presents the 95% confidence intervals of the posterior estimates for each model parameter across all catchments. These intervals are used to assess the influence of each driver on variation in the C-Q slope. In particular, a 95% confidence interval that does not cross the zero line indicates that the corresponding driver has a clear positive or negative effect on the C–Q slope (i.e., it either steepens or flattens the relationship). Following this, fire occurrence (represented by $\beta_{S,if\_afterfire}$ in Eqn. 3) has a clear positive effect of event-scale C-Q slopes for five catchments 208004, 208011, 208009, 212058 and 215215 (Fig. 6a). Notably, all five catchments are amongst catchments with >0.1% of catchment areas experienced extreme burning. Further, two of the five catchments are also the two most extremely burnt catchments studied (i.e., 212058 and 21515) with 14.2%, 15.2% catchment area experienced extreme burning, respectively.

The other catchments with less extreme burning (<10% catchment area), along with the non-extremely burnt catchments, did not see a consistent post-fire increase in event C-Q slopes. This might mean that fire has not had clear impacts on sediment export, or could alternatively be a result of the potential interaction between effects of fire and short-term hydrologic conditions which shape the C-Q slopes together.

https://doi.org/10.5194/egusphere-2025-6244
Preprint. Discussion started: 19 February 2026

3.2.2 The dominant driver of event C-Q slopes

The current event volume ($\beta_{S,Q_{thisvolume}}$ in Eq. 3) has clear positive effects on C-Q slopes for 4 out of the 14 catchments, and clear negative effects for 6 catchments (Fig. 6b). The last event volume ($\beta_{S,Q_{lastvolume}}$ in Eq. 3) has clear positive effects on C-Q slopes for 5 out of the 14 catchments, and clear negative effects for another 6 catchments. The time since last event ($\beta_{S,timesincelast}$ in Eq. 3) has clear positive effects on C-Q slopes for 6 out of the 14 catchments, and clear negative effects for another 6 catchments.

However, looking across the posterior distributions of the three parameters describing short-term hydrological influences (i.e., current and last event volume, and time since last event) – specifically how far each box deviates from the zero line (Fig. 6b-d) – we see the impacts of these short-term hydrologic conditions on the C-Q slopes are notably smaller compared to the modelled effect of fire shown in Fig. 6a. This suggests that extreme burning is likely a primary driver of shifts in catchment sediment export, compared with hydrologic drivers.

Focusing on the fire effects of individual catchments (represented by each box in Fig. 6a), while catchments are ordered along the x-axis by fire severity in Fig. 6a, their fire effects do not appear to always follow a monotonic change with their burning severities. For example, the third most severely burnt catchments (212042) did not even experience an increase in the post-fire C-Q slopes; in contrast, some less severely burnt catchments (208004, 208011, 208009) demonstrated clear increases in the post-fire C-Q slopes. These suggest the effect of fire on sediment mobilization may vary beyond a simple function of burning severity, demonstrating the potential modulation effects by other catchment features. As such, the subsequent analysis further explores how these fire effects change across space with burning characteristics and other catchment geographic features.

https://doi.org/10.5194/egusphere-2025-6244
Preprint. Discussion started: 19 February 2026

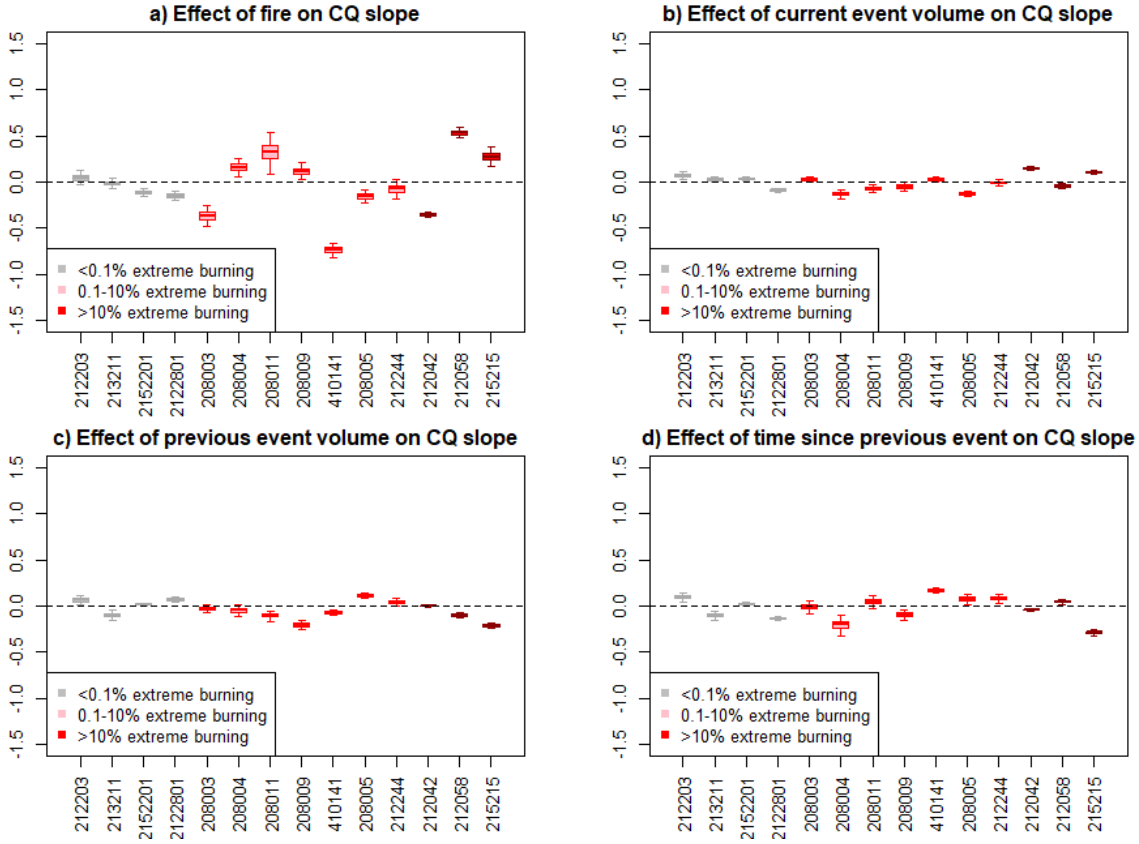

Figure 6: Modelled effects of a) if after fire; b) total flow volume over current storm event; c) total flow volume over previous storm event; d) time since previous storm event, on event C-Q slopes. Each box shows the posterior distribution (with whiskers extending to the 95% confidence interval) of each model parameter, for a specific catchment within the 14 analyzed, ordered by the percentage area being extremely burnt. A box with whiskers not overlapping with the dotted zero-line indicates a strong positive effect (i.e., increase in the specific indicator leads to a more positive event C-Q slope) or strong negative effect (i.e., increase in the specific indicator leads to a more negative event C-Q slope).

3.2.3 How does the impact of fire on event C-Q slopes change across catchments

Fig. 7 explores how the post-fire shift in C-Q slope (expressed as the mean of posterior $\beta_{S,if\_afterfire}$ in Eqn. 3 for each catchment) changes across the 10 extremely burnt catchments.

A correlation analysis with the full list of catchment characteristics (including geography, burning characteristics and forest formation types, see Table 3) revealed that the post-fire shift in C-Q slopes are not significantly correlated with any catchment characteristics (Fig. A2, Appendix A), highlighting the potentially complex spatial patterns driving these effects. The scatterplots in Fig. 7 shows the post-fire shift in C-Q slope (in the y-axis) against each of the six catchment characteristics (x-

https://doi.org/10.5194/egusphere-2025-6244
Preprint. Discussion started: 19 February 2026

axes) which have the highest Pearson correlation coefficients with these shifts. The post-fire shifts in C-Q slopes appears to follow a clear negative relationship with each of the percentage catchment cover with Eucalyptus medium open forest (Pearson's ρ=-0.53) and the normalized distance to outlet (Pearson's ρ=-0.52). These suggest that we generally see greater post-fire increases in C-Q slopes in catchments where 1) the extreme burning is closer to the catchment outlet; and 2) the percentage coverage of Eucalyptus medium open forest is lower.

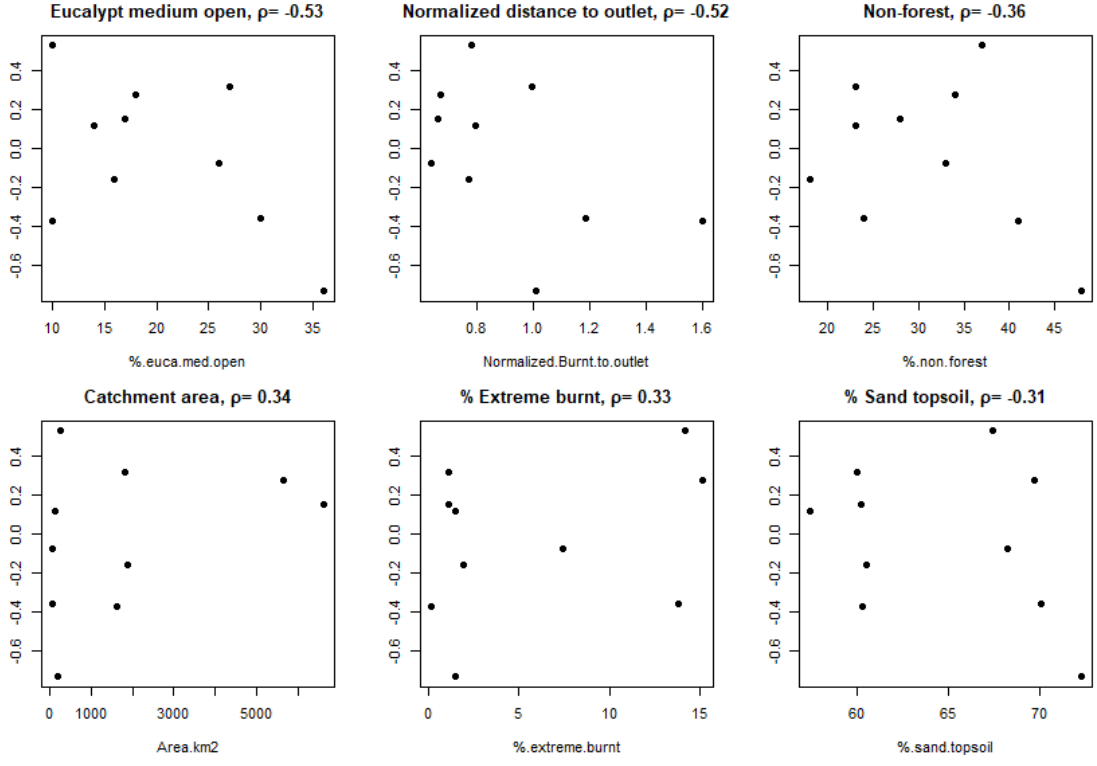

Figure 7: Scatter plots of the post-fire shift in C-Q slope ($\beta_{S,if\_afterfire}$, y-axis) for the 10 extremely burnt catchments, against the six catchment characteristics showing strongest correlation with the post-fire C-Q shift (x-axis of each panel). Each panel title specifies the Pearson correlation coefficient between the post-fire shift in C-Q slope and the specific catchment characteristics. Note that only catchment characteristics with a Pearson's correlation ≥ 0.3 with the post-fire shift in C-Q slope are presented, and the full correlation results are shown in Fig. A2, Appendix A.

The remaining key spatial drivers of the post-fire shifts in C-Q slopes all have weaker correlations with the post-fire shifts in C-Q slopes. These are, specifically, percentage of non-forest cover (Pearson's ρ=-0.36), catchment area (Pearson's ρ=0.34), percentage catchment being extremely burnt (Pearson's ρ=0.33) and percentage catchment topsoil composed by sand (Pearson's ρ=-0.31). Notably, there are substantial scatters in the relationships between each of these characteristics and the post-fire shifts in C-Q slopes indicating their weaker effects. For example, the positive correlations for the percentage

https://doi.org/10.5194/egusphere-2025-6244
Preprint. Discussion started: 19 February 2026

catchment being extremely burnt and the catchment area, both seem to be largely driven by the cluster of data points with smaller x values close to 0.

4 Discussions

4.1 Hydrological and sedimentological changes in forested catchments following fire from the literature

In forested catchments, the hydrologic and geomorphic consequences of wildfire are pronounced. The impacts of forest fires include reduced canopy interception and evapotranspiration, increased nutrient losses, and enhanced soil erosion (Meyer et al., 2001; Nolan et al., 2014; Khaledi et al., 2022). Subsequent rainfall interacts with the modified soil–vegetation–landscape system, frequently producing shifts in the generation of runoff and sediment loads. Several mechanisms have been proposed to explain these changes (Shakesby, 2011), including: (1) the generation of additional sediment sources through vegetation and litter loss; (2) changes to soil cover and structure; (3) altered hydrophobic properties of surface soils; and (4) reduced root-mitigated soil cohesion due to fire-induced vegetation mortality.

Severe burning can expose bare mineral soils and destabilise hillslopes by removing vegetation cover and litter layers that protect the soil from raindrop impact. The loss of near-surface root structures further reduces soil cohesion, making soils more susceptible to detachment and transport (Nyman et al., 2020). These processes collectively create new and spatially distributed sediment sources within the catchment. In particular, high-severity fires can promote the formation of rills and gullies and increase the likelihood of channel bank erosion, substantially expanding the area contributing to sediment mobilization (Alessio et al., 2021).

Extreme severity of fires may also reduce hydrophobicity through the destruction of organic coatings on soil particles (Caltabellotta et al., 2022). However, this effect is often masked by the highly heterogeneous patterns of fire severity observed at the catchment scale, for which the infiltration and runoff responses may be highly spatially variable for the hydrophobicity effects to be measured or analytically recognized (Woods et al., 2007).

The hydrologic consequences of wildfire are commonly observed through increased runoff-to-rainfall ratios (Nolan et al., 2014). Following fire, the combination of reduced evapotranspiration, the filling of macropores with ash and debris, and the possible development of hydrophobic soil layers can enhance direct runoff generation (Balfour et al., 2014). Catchments that shift toward Hortonian overland flow exhibit faster and higher-magnitude hydrologic responses to rainfall events, which, in turn, elevate sediment mobilization and turbidity during the early phases of post-fire runoff.

The material contributing to post-fire turbidity typically consists of a mixture of soil particles, ash, and organic detritus. These materials are more readily entrained and transported after burning due to the loss of vegetation and structural protection on hillslopes (Woods and Balfour, 2008). Such fine and light particles are easily mobilized even under moderate rainfall events, sustaining elevated turbidity levels over multiple storm events.

https://doi.org/10.5194/egusphere-2025-6244
Preprint. Discussion started: 19 February 2026

4.2 Plausible driving mechanisms revealed by our analyses

The changes in the hydrological and sedimentological behaviour of catchments following bushfires, as described above, cannot be attributed to any single, or a single set, of the mechanisms proposed in literature. However, our analysis suggests some mechanisms are more likely.

The 10 extremely burnt catchments examined here show substantial variability in how the sediment C-Q relationship changed after fire, pointing to heterogeneous shifts in sediment mobilization processes rather than a consistent post-fire change. While our results show that fire and hydrologic variability collectively determine both the availability of sediment sources and the efficiency of hydrologic connectivity that delivers sediment to streams. Notably, extreme burning appears to play a more critical role than short-term hydrologic conditions in controlling catchment-scale sediment export following fire.

While several catchments that experienced extreme burning exhibited clear increases in C-Q slopes – which suggests possibly enhanced sediment availability and potential changes in the soil cover and structure making it more prone to erosion – this steepening of C-Q slopes was far from universal across catchments. The behaviours shown in Fig. 6 emphasize that post-fire water-quality responses cannot be inferred solely from burn severity. Fig. 7 further flags that the post-fire changes in sediment mobilization appear to be strongly modulated by catchment characteristics such as forest formation type (including vegetation type, covering and height) and the proximity of extremely burnt areas to the catchment outlet (where flow and turbidity measurements were taken). This contrasts with the consistently reported upward shift in the C-Q slope post fire in literature (Johnston and Maher 2022; Richardson et al. 2024; Clow et al. 2024). Our findings highlight the potential interplay between burn severity and the underlying geomorphic and vegetation context in jointly shaping the mobilisation of sediments in catchments.

4.3 Limitations

The purpose of our modelling is to assess impacts of severe fire occurrence and short-term hydrological conditions on sediment mobilization. To focus on this, we have intentionally kept the model structure parsimonious (i.e., with Eqn. 3) and have not explicitly considered any secondary interactions of:

1. Interaction between the fire and hydrological conditions (e.g., possible changes in rainfall-runoff ratio before and after fire), given the coinciding flooding conditions during the post-fire periods. This is broadly demonstrated with Fig. 2 c and d), but further event-scale assessment would be warranted where the focus is on hydrological changes.
2. We have also assumed that the effect of short-term hydrological conditions (i.e.., β terms in Eqn. 3) on the event C-Q slopes remains stationary over time. Fig. 8 presents a preliminary analysis on this, where the correlations between the current event volume and event C-Q slope shows a systematic post-fire shift across catchments; however, the fact that such shift is also notable for non-extremely burnt catchment suggests other possible mechanisms explaining the shift e.g., the flooding condition post the fire period. Further study is required to untangle such temporally varying effects of hydrologic conditions on the event C-Q slopes.

https://doi.org/10.5194/egusphere-2025-6244
Preprint. Discussion started: 19 February 2026

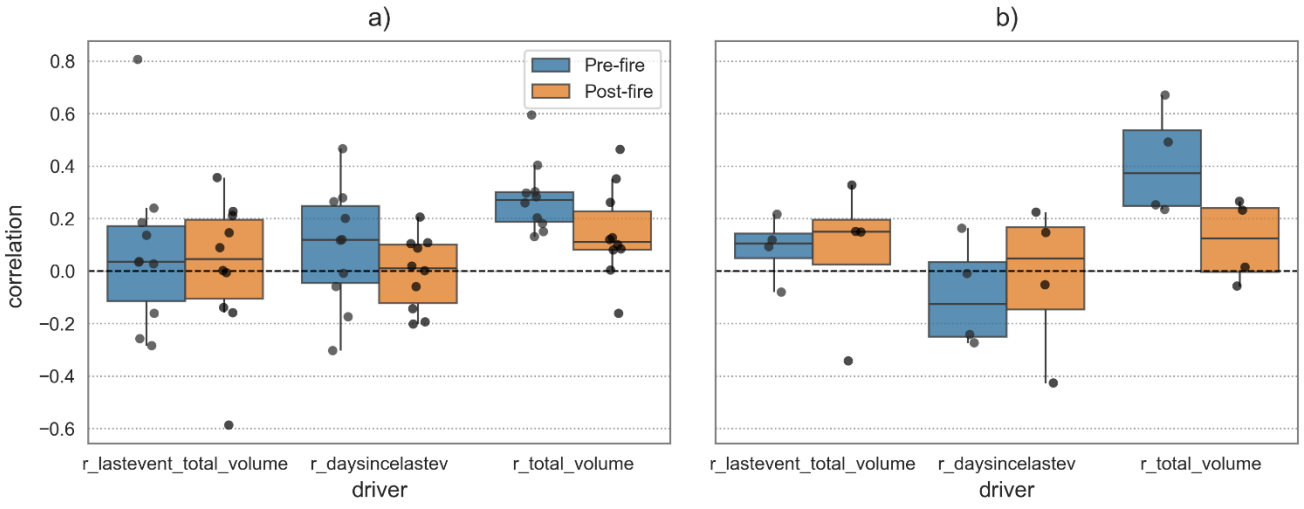

Figure 8: Distribution of the correlation of event C-Q slopes across a) the extremely burnt catchments; and b) non-extremely burnt catchments, with the three model predictors included in Eqn. 3: *lastevent_total_volume* – total flow volume of last storm event; *daysincelastev* – days since last storm event (till the start of the current event); *total_volume* – total flow volume of the current storm event. The colours separate the pre- and post-fire periods for each predictor where correlation was analyzed.

5 Conclusions

Numerous studies have investigated the impact of fire on water quality. However, a multi-catchment, event-scale analysis is still lacking, largely owed to the limitation of high-frequency monitoring data in history. Our study fills this gap with a multi-year, high-frequency turbidity and streamflow data collected from 14 forested catchments in eastern Australia burned to varying severities during the 2019/2020 Black Summer fires and affected by subsequent floods. Our focus was to understand the effects of fire and short-term hydrologic conditions, and the spatial patterns of these effects.

Our study suggests that extreme burning appears to be a primary driver of post-fire changes in sediment mobilization, compared with short-term hydrologic conditions, and the locations of extreme burning and forest type are critically linked to the magnitude of these post-fire changes. Our results revealed how catchment characteristics, landcover and hydroclimate conditions work together in modulating the post-fire sediment responses, across varying catchment characteristics and burning severities. Future work could dive into the temporal variation of such post-fire sediment responses, identify shifts to recovery period and explore how this varies across regions.

https://doi.org/10.5194/egusphere-2025-6244
Preprint. Discussion started: 19 February 2026

Code and data availability

All data used in this study were gathered from public repositories detailed in Sect. 2.1. The modelling code is included in Fig. A2, Appendix A.

Author contributions

DG – conceptualization, data curation, formal analysis, investigation, methodology, resources, supervision, software, validation, visualization, writing (original draft preparation, review and editing). QW – conceptualization, data curation, formal analysis, investigation, methodology, validation, visualization, writing (original draft preparation, review and editing). PBH – conceptualization, methodology, resources, writing (original draft preparation, review and editing).

Competing interests

The authors declare that they have no conflict of interest.

https://doi.org/10.5194/egusphere-2025-6244
Preprint. Discussion started: 19 February 2026

References

Alessio, P., Dunne, T., & Morell, K. (2021). Post-wildfire generation of debris-flow slurry by rill erosion on colluvial hillslopes. *Journal of Geophysical Research: Earth Surface*, 126, e2021JF006108. https://doi.org/10.1029/2021JF006108

Australian Bureau of Agricultural and Resource Economics and Sciences (ABARES), Forests of Australia (2018), Australian Bureau of Agricultural and Resource Economics and Sciences, Canberra, December. CC BY 4.0. www.doi.org/10.25814/5c59170ec780d

Balfour, V.N., Doerr, S.H. and Robichaud, P.R. (2014). The temporal evolution of wildfire ash and implications for post-fire infiltration. *International Journal of Wildland Fire*, 23(5), pp.733-745

Brown, E. and Hunt, B. P. V. (2025). Cumulative effects of fire in the Fraser River basin on freshwater quality and implications for the Salish Sea, *Science of The Total Environment*, 978, 179416, https://doi.org/10.1016/j.scitotenv.2025.179416.

Caltabellotta, G., Iovino, M. and Bagarello, V., (2022). Intensity and persistence of water repellency at different soil moisture contents and depths after a forest wildfire. *Journal of Hydrology and Hydromechanics*, *70*(4), pp.410-420.

Cerdà, A. and Doerr, S.H., (2008). The effect of ash and needle cover on surface runoff and erosion in the immediate post-fire period. *Catena*, *74*(3), pp.256-263.

Chen, J. and Chang, H. (2023): A review of wildfire impacts on stream temperature and turbidity across scales, *Progress in Physical Geography: Earth and Environment*, 47, 369–394, https://doi.org/10.1177/03091333221118363.

Clow, D. W., Akie, G. A., Murphy, S. F., and Gohring, E. J. (2024): Dynamic water-quality responses to wildfire in Colorado, *Hydrological Processes*, 38, e15291, https://doi.org/10.1002/hyp.15291.

Collins, L., Bradstock, R. A., Clarke, H., Clarke, M. F., Nolan, R. H., & Penman, T. D. (2021). The 2019/2020 mega-fires exposed Australian ecosystems to an unprecedented extent of high-severity fire. *Environmental Research Letters*, 16(4), 044029. https://doi.org/10.1088/1748-9326/abeb9e

Cunningham, C.X., Williamson, G.J. & Bowman, D.M.J.S. (2024). Increasing frequency and intensity of the most extreme wildfires on Earth. *Nat Ecol Evol* 8, 1420–1425. https://doi.org/10.1038/s41559-024-02452-2

Department of Industry, Science, Energy and Resources (2019). National forest and sparse woody vegetation data. Version 4.0. Commonwealth of Australia, Canberra. Available from: https://data.gov.au/data/dataset/5176de70-d559-40ae-b061-7291e27e687b. Accessed 1/10/2025.

Doerr, S.H., Shakesby, R.A., Blake, W.H., Chafer, C.J., Humphreys, G.S. and Wallbrink, P.J., (2006). Effects of differing wildfire severities on soil wettability and implications for hydrological response. *Journal of Hydrology*, *319*(1-4), pp.295-311.

Dupas, R., Causse, J., Jaffrezic, A., Aquilina, L., and Durand, P.: Flowpath controls on high-spatial-resolution water-chemistry profiles in headwater streams, *Hydrol. Process.*, 35, e14247, https://doi.org/10.1002/hyp.14247, 2021.

Ebeling, P., Kumar, R., Weber, M., Knoll, L., Fleckenstein, J. H., and Musolff, A. (2021): Archetypes and Controls of Riverine Nutrient Export Across German Catchments, *Water Resour. Res.*, 57, e2020WR028134, https://doi.org/10.1029/2020WR028134.

https://doi.org/10.5194/egusphere-2025-6244
Preprint. Discussion started: 19 February 2026

Gallant, J., Wilson, N., Dowling, T., Read, A., Inskeep, C. (2011). SRTM-derived 1 Second Digital Elevation Models Version 1.0. 1. Geoscience Australia, Canberra. Available from: https://pid.geoscience.gov.au/dataset/ga/72759. Accessed 01/07/2024.

Gorski, G. and Zimmer, M. A. (2021): Hydrologic regimes drive nitrate export behavior in human-impacted watersheds, *Hydrol. Earth Syst. Sci.*, 25, 1333–1345, https://doi.org/10.5194/hess-25-1333-2021.

Guo, D., Lintern, A., Webb, J. A., Ryu, D., Liu, S., Bende-Michl, U., Leahy, P., Wilson, P., and Western, A. W. (2019): Key Factors Affecting Temporal Variability in Stream Water Quality, *Water Resour. Res.*, 55, 112–129, https://doi.org/10.1029/2018wr023370.

Guo, D., Lintern, A., Webb, J. A., Ryu, D., Bende-Michl, U., Liu, S., and Western, A. W. (2020): A data-based predictive model for spatiotemporal variability in stream water quality, *Hydrol. Earth Syst. Sci.*, 24, 827–847, https://doi.org/10.5194/hess-24-827-2020.

Guo, D., Minaudo, C., Lintern, A., Bende-Michl, U., Liu, S., Zhang, K., & Duvert, C. (2022). Synthesizing the impacts of baseflow contribution on concentration–discharge (C–Q) relationships across Australia using a Bayesian hierarchical model. *Hydrol. Earth Syst. Sci.*, 26(1), 1-16. https://doi.org/10.5194/hess-26-1-2022

Guo, D., Saft, M., Hou, X., Webb, J. A., Hairsine, P. B., & Western, A. W. (2023). How does wildfire and climate variability affect streamflow in forested catchments? A regional study in eastern Australia. *Journal of Hydrology*, 625, 129979. https://doi.org/https://doi.org/10.1016/j.jhydrol.2023.129979

Hall, N., Rust, A., Hogue, T. S., and Singha, K. (2022): Analysis of watershed parameters controlling turbidity following the West Fork Complex fire, *Journal of Hydrology*, 609, 127712, https://doi.org/10.1016/j.jhydrol.2022.127712.

Hampton, T. B., Lin, S., & Basu, N. B. (2022). Forest fire effects on stream water quality at continental scales: a meta-analysis. *Environmental Research Letters*, 17(6), 064003. https://doi.org/10.1088/1748-9326/ac6a6c

Jaffrés, J. B. D., Cuff, B., Cuff, C., Faichney, I., Knott, M., & Rasmussen, C. (2021). Hydrological characteristics of Australia: relationship between surface flow, climate and intrinsic catchment properties. *Journal of Hydrology*, 603, 126911. https://doi.org/https://doi.org/10.1016/j.jhydrol.2021.126911

Jensen, C. K., McGuire, K. J., McLaughlin, D. L., and Scott, D. T. (2019): Quantifying spatiotemporal variation in headwater stream length using flow intermittency sensors, *Environ. Monit. Assess.*, 191, 226, https://doi.org/10.1007/s10661-019-7373-8.

Johnston, S. G. and Maher, D. T. (2022): Drought, megafires and flood - climate extreme impacts on catchment-scale river water quality on Australia's east coast, *Water Research*, 218, 118510, https://doi.org/10.1016/j.watres.2022.118510.

Kemter, M., Fischer, M., Luna, L. V., Schönfeldt, E., Vogel, J., Banerjee, A., et al. (2021). Cascading hazards in the aftermath of Australia's 2019/2020 Black Summer wildfires. *Earth's Future*, 9, e2020EF001884. https://doi.org/10.1029/2020EF001884

Khaledi, J., Lane, P. N. J., Nitschke, C. R., & Nyman, P. (2022). Wildfire contribution to streamflow variability across Australian temperate zone. *Journal of Hydrology*, 609, 127728. https://doi.org/https://doi.org/10.1016/j.jhydrol.2022.127728

https://doi.org/10.5194/egusphere-2025-6244
Preprint. Discussion started: 19 February 2026

Knapp, J. L. A., von Freyberg, J., Studer, B., Kiewiet, L., and Kirchner, J. W. (2020): Concentration–discharge relationships vary among hydrological events, reflecting differences in event characteristics, *Hydrol. Earth Syst. Sci.*, 24, 2561–2576, https://doi.org/10.5194/hess-24-2561-2020.

Kuczera, G. (1987). Prediction of water yield reductions following a bushfire in ash-mixed species eucalypt forest. *Journal of Hydrology* 94 (3–4), 215–236.

Ladson, A., Brown, R., Neal, B., & Nathan, R. (2013). A standard approach to baseflow separation using the Lyne and Hollick filter. *Australian Journal of Water Resources*, 17(1).

Malone, Brendan; & Searle, Ross (2022): Soil and Landscape Grid National Soil Attribute Maps - Sand (3" resolution) - Release 2. v4. CSIRO. Data Collection. https://doi.org/10.25919/rjmy-pa10

McGuire, K. J., Torgersen, C. E., Likens, G. E., Buso, D. C., Lowe, W. H., and Bailey, S. W.: Network analysis reveals multiscale controls on streamwater chemistry, *P. Natl. Acad. Sci. USA*, 111, 7030–7035, https://doi.org/10.1073/pnas.1404820111, 2014.

Marcotte, A. L., Limpens, J., Nunes, J. P., Howard, B. C., Hurley, A. G., Khamis, K., Krause, S., Croghan, D., Kourmouli, A., Leader, S., Singh, T., Stoof, C. R., Ullah, S., and Kettridge, N. (2024): Enhanced Hydrologic Connectivity and Solute Dynamics Following Wildfire and Drought in a Contaminated Temperate Peatland Catchment, Water Resources Research, 60, e2023WR036412, https://doi.org/10.1029/2023WR036412.

Mast, M. A., Murphy, S. F., Clow, D. W., Penn, C. A., and Sexstone, G. A. (2016): Water-quality response to a high-elevation wildfire in the Colorado Front Range, Hydrological Processes, 30, 1811–1823, https://doi.org/10.1002/hyp.10755.

Minaudo, C., Dupas, R., Gascuel-Odoux, C., Roubeix, V., Danis, P.-A., and Moatar, F. (2019): Seasonal and event-based concentrationdischarge relationships to identify catchment controls on nutrient export regimes, *Adv. Water Resour.*, 131, 103379, https://doi.org/10.1016/j.advwatres.2019.103379.

Moatar, F., Floury, M., Gold, A. J., Meybeck, M., Renard, B., Ferréol, M., Chandesris, A., Minaudo, C., Addy, K., Piffady, J., and Pinay, G. (2020): Stream Solutes and Particulates Export Regimes: A New Framework to Optimize Their Monitoring, *Frontiers in Ecology and Evolution*, 7, 516, https://doi.org/10.3389/fevo.2019.00516, 2020.

Mohammadpour Khoie, M. M., Guo, D., & Wasko, C. (2025). Improving the consistency of hydrologic event identification. *Environmental Modelling & Software*, 191, 106521. https://doi.org/https://doi.org/10.1016/j.envsoft.2025.106521

Nolan, R.H., Lane, P.N., Benyon, R.G., Bradstock, R.A. and Mitchell, P.J. (2014). Changes in evapotranspiration following wildfire in resprouting eucalypt forests. *Ecohydrology*, *7*(5), pp.1363-1377.

Nyman, P., Sheridan, G.J., Smith, H.G. and Lane, P.N. (2014). Modeling the effects of surface storage, macropore flow and water repellency on infiltration after wildfire. *Journal of Hydrology*, *513*, pp.301-313.

Nyman, P., Box, W.A., Stout, J.C., Sheridan, G.J., Keesstra, S.D., Lane, P.N. and Langhans, C. (2020). Debris-flow-dominated sediment transport through a channel network after wildfire. *Earth Surface Processes and Landforms*, *45*(5), pp.1155-1167.

https://doi.org/10.5194/egusphere-2025-6244
Preprint. Discussion started: 19 February 2026

NSW Government and NSW Department of Climate Change, Energy, the Environment and Water (DCCEEW) (2020a), Fire Extent and Severity Mapping (FESM) 2019/20. Available from: https://datasets.seed.nsw.gov.au/dataset/f7eb3f73-5831-4cc9-8259-8d1f210214ac. Accessed 01/07/2024.

NSW Government and NSW Department of Climate Change, Energy, the Environment and Water (DCCEEW) (2020b), Fire Extent and Severity Mapping (FESM) 2018/19. Available from: https://datasets.seed.nsw.gov.au/dataset/c2427005-febe-4e4e-a300-2c4ddd0066be. Accessed 01/07/2024.

NSW Government and NSW Department of Climate Change, Energy, the Environment and Water (DCCEEW) (2021), Fire Extent and Severity Mapping (FESM) 2017/18. Available from: https://datasets.seed.nsw.gov.au/dataset/6ff6aedc-5131-4667-ac34-e9d9aa8aeb99. Accessed 01/07/2024.

Raoelison, O. D., Valenca, R., Lee, A., Karim, S., Webster, J. P., Poulin, B. A., & Mohanty, S. K. (2023). Wildfire impacts on surface water quality parameters: Cause of data variability and reporting needs. *Environmental Pollution*, 317, 120713. https://doi.org/https://doi.org/10.1016/j.envpol.2022.120713

Reale, J. K., Van Horn, D. J., Condon, K. E., and Dahm, C. N. (2015): The effects of catastrophic wildfire on water quality along a river continuum, *Freshwater Science*, 34, 1426–1442, https://doi.org/10.1086/684001.

Rhoades, C. C., Entwistle, D., Butler, D. (2011) The influence of wildfire extent and severity on streamwater chemistry, sediment and temperature following the Hayman Fire, ColoradoA. *International Journal of Wildland Fire*, 20, 430–442. https://doi.org/10.1071/WF09086

Richardson, C., Montalvo, M., Wagner, S., Barton, R., Paytan, A., Redmond, M., and Zimmer, M. (2024): Exploring the complex effects of wildfire on stream water chemistry: insights from concentration-discharge relationships, *Water Resources Research*, 60, e2023WR034940, https://doi.org/10.1029/2023WR034940.

Shakesby, R.A.(2011). Post-wildfire soil erosion in the Mediterranean: Review and future research directions. *Earth-Science Reviews*, *105*(3-4), pp.71-100.

Rust, A. J., Hogue, T. S., Saxe, S., and McCray, J. (2018): Post-fire water-quality response in the western United States, *Int J Wildland Fire*, 27, 203–216, https://doi.org/10.1071/WF17115.

Sherson, L. R., Van Horn, D. J., Gomez-Velez, J. D., Crossey, L. J., and Dahm, C. N. (2015): Nutrient dynamics in an alpine headwater stream: use of continuous water quality sensors to examine responses to wildfire and precipitation events, *Hydrological Processes*, 29, 3193–3207, https://doi.org/10.1002/hyp.10426.

Smith, H. G., Sheridan, G. J., Lane, P. N. J., Nyman, P., and Haydon, S. (2011): Wildfire effects on water quality in forest catchments: A review with implications for water supply, *Journal of Hydro*logy, 396, 170–192, https://doi.org/10.1016/j.jhydrol.2010.10.043.

Stan Development Team (2025). "RStan: the R interface to Stan." R package version 2.32.7, https://mc-stan.org/.

Tunqui Neira, J. M., Andréassian, V., Tallec, G., and Mouchel, J.-M. (2020a): Technical note: A two-sided affine power scaling relationship to represent the concentration–discharge relationship, *Hydrol. Earth Syst. Sci.*, 24, 1823–1830, https://doi.org/10.5194/hess-24-1823-2020.

https://doi.org/10.5194/egusphere-2025-6244
Preprint. Discussion started: 19 February 2026

Tunqui Neira, J. M., Tallec, G., Andréassian, V., and Mouchel, J.-M. (2020b): A combined mixing model for high-frequency concentration–discharge relationships, J. Hydrol., 591, 125559, https://doi.org/10.1016/j.jhydrol.2020.125559.

Vertessy, R.A., Watson, F.G.R., O'Sullivan, S.K., (2001). Factors determining relations between stand age and catchment water balance in mountain ash forests. *Forest Ecology and Management* 143 (1), 13–26. https://doi.org/10.1016/S0378-1127(00) 00501-6.

Wasko, C., & Guo, D. (2022). Understanding event runoff coefficient variability across Australia using the hydroEvents R package. *Hydrological Processes*, 36(4), e14563. https://doi.org/10.1002/hyp.14563

WaterNSW (2020). Continuous water monitoring network. Available from: https://realtimedata.waternsw.com.au/water.stm. Accessed 01/07/2024.

Webb, A.A., Jarrett, B.W., (2013) Hydrological response to wildfire, integrated logging and dry mixed species eucalypt forest regeneration: The Yambulla experiment. *Forest ecology and management* 306, 107–117. https://doi.org/10.1016/j.foreco.2013.06.020.

Webb, J. A. and King, L. E. (2009): A Bayesian hierarchical trend analysis finds strong evidence for large-scale temporal declines in stream ecological condition around Melbourne, Australia, *Ecography*, 32, 215–225, https://doi.org/10.1111/j.1600-0587.2008.05686.x.

Woods, S.W. and Balfour, V.N. (2008). The effect of ash on runoff and erosion after a severe forest wildfire, Montana, USA. *International Journal of Wildland Fire*, 17(5), pp.535-548.

Woods, S.W., Birkas, A. and Ahl, R. (2007). Spatial variability of soil hydrophobicity after wildfires in Montana and Colorado. *Geomorphology*, *86*(3-4), pp.465-479.

https://doi.org/10.5194/egusphere-2025-6244
Preprint. Discussion started: 19 February 2026

Appendix A

Figure A1. Rstan codes for the full Bayesian hierarchical model described in Sect. 2.3.

```
data {
  int<lower=1> N; //the total number of observations
  int<lower=1> Ntotevents; //the total number of events
  int<lower=1> Nsites; //the total number of catchments

  vector[N] C; //all C data during events (untransformed)
  vector[N] Q; //all Q data during events (untransformed)

  array[N] int<lower=1> toteventid;  // event id for each observation (1..Ntotevents)

  array[Ntotevents] int<lower=1> siteid;  // site id for each event (1..Nsites)
  vector[Ntotevents] lastvolume;//
  vector[Ntotevents] thisvolume;//
  vector[Ntotevents] timesincelast;
  vector[Ntotevents] if_afterfire;
}
parameters {
  real<lower=0> sign;                     // global standard deviation for all
observations
  vector[Nsites] inter_be;                // site-level intercept for the regression
for beta

  vector[Nsites] mu_alpha;                // site-level mean of alpha
  vector<lower=0>[Nsites] sigma_alpha;    // site-level SD of alpha
  vector[Ntotevents] z_alpha;             // standard normals for site-level alpha (one
per event)
  vector<lower=0>[Nsites] tau;            // site SDs for alpha

  vector[Nsites] Beta_lastvolume;         // model parameters for each of four
predictors of event C-Q slopes
  vector[Nsites] Beta_thisvolume;
  vector[Nsites] Beta_timesincelast;
  vector[Nsites] Beta_afterfire;

  real mu_beta_lastvolume;                // hyper-parameters for the above four
parameters
  real<lower=0> sig_beta_lastvolume;
  real mu_beta_thisvolume;
  real<lower=0> sig_beta_thisvolume;
  real mu_beta_timesincelast;
  real<lower=0> sig_beta_timesincelast;
  real mu_beta_afterfire;
  real<lower=0> sig_beta_afterfire;
}
transformed parameters {
  vector[N] Chat;                         // modelled concentrations (as log10 NTU
Turbidity)

  vector[Ntotevents] alpha = mu_alpha[siteid] + tau[siteid] .* z_alpha; // modelling
event-scale alpha
  vector[Ntotevents] beta =                                             // modelling
event-scale beta (Eqn. 3)
      inter_be[siteid]
    + Beta_lastvolume[siteid] .* lastvolume
    + Beta_thisvolume[siteid] .* thisvolume
    + Beta_timesincelast[siteid] .* timesincelast
    + Beta_afterfire[siteid] .* if_afterfire;

    Chat = alpha[toteventid] + beta[toteventid] .* log10(Q);            // classic
power-law CQ (Eqn. 2)
}
model {
    tau ~ exponential(1);                 // half-normal-ish on positive scale

    mu_alpha ~ normal(0,1);
    z_alpha ~ normal(0,1);

    inter_be ~ normal(0,1);
```

https://doi.org/10.5194/egusphere-2025-6244
Preprint. Discussion started: 19 February 2026

```
    mu_beta_lastvolume ~ normal(0,1);     // pooled effects - common mean of each
parameter value across sites
    mu_beta_thisvolume ~ normal(0,1);
    mu_beta_timesincelast ~ normal(0,1);
    mu_beta_afterfire ~ normal(0,1);

    sig_beta_lastvolume ~ exponential(1); // pooled effects - common stdev. of each
parameter value across sites
    sig_beta_thisvolume ~ exponential(1);
    sig_beta_timesincelast ~ exponential(1);
    sig_beta_afterfire ~ exponential(1);

    Beta_lastvolume ~ normal(mu_beta_lastvolume,sig_beta_lastvolume); // Pooling
(information sharing across sites)
    Beta_thisvolume ~ normal(mu_beta_thisvolume,sig_beta_thisvolume);
    Beta_timesincelast ~ normal(mu_beta_timesincelast,sig_beta_timesincelast);
    Beta_afterfire ~ normal(mu_beta_afterfire,sig_beta_afterfire);


    sign ~ student_t(4, 0, 1);           // residual on modelled y
    log10(C) ~ normal(Chat,sign) ;

}
generated quantities {
  vector[N] log_lik;

    for ( n in 1:N ) {
      log_lik[n] = normal_lpdf(log10(C[n]) |Chat[n], sign);

     }
}
```

580

https://doi.org/10.5194/egusphere-2025-6244
Preprint. Discussion started: 19 February 2026

Figure A2. Cross-correlation of the modelled fire effects with catchment geography, burning characteristics and forest formation. The Pearson correlation coefficients are presented for each pair of variables which exhibit significant correlation at p<0.05, while coefficients of non-significant correlation are not shown.

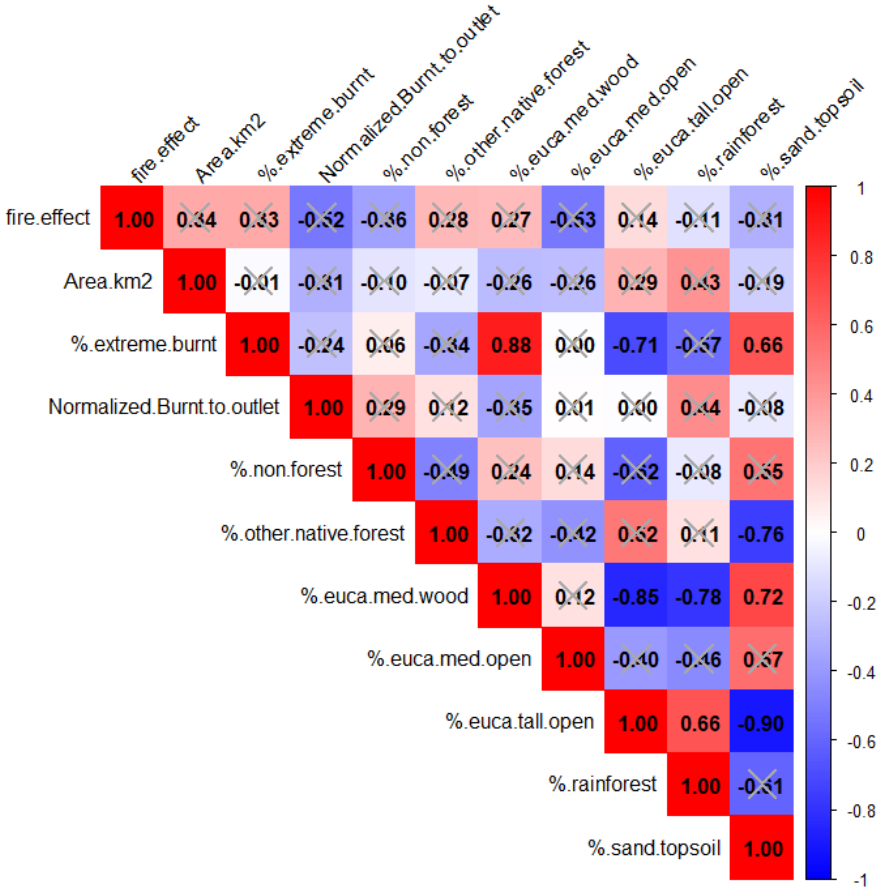

585